High temperature creep behaviour of Al-rich Ti-Al alloys

Journal of Physics: Conference Series **240** (2010) 012084 doi:10.1088/1742-6596/240/1/012084

High temperature creep behaviour of Al-rich Ti-Al alloys

D Sturm[1], M Heilmaier[1], H Saage[1], J Aguilar[2], G J Schmitz[2], A Drevermann[2], M Palm[3], F Stein[3], N Engberding[3], K Kelm[4], S Irsen[4]

[1] Otto von Guericke University Magdeburg, Institute for Materials and Joining Technology, P.O. Box 4120, D-39016 Magdeburg, Germany
[2] ACCESS e.V., Intzestraße 5, D-52072 Aachen, Germany
[3] Max-Planck-Institut für Eisenforschung GmbH, Max-Planck-Str. 1, D-40237 Düsseldorf, Germany
[4] Stiftung caesar, Electron Microscopy, Ludwig-Erhard-Allee 2, D-53175 Bonn, Germany

daniel.sturm@ovgu.de

Abstract. Compared to Ti-rich γ-TiAl-based alloys Al-rich Ti-Al alloys offer an additional reduction of in density and a better oxidation resistance which are both due to the increased Al content. Polycrystalline material was manufactured by centrifugal casting. Microstructural characterization was carried out employing light-optical, scanning and transmission electron microscopy and XRD analyses. The high temperature creep of two binary alloys, namely $Al_{60}Ti_{40}$ and $Al_{62}Ti_{38}$ was comparatively assessed with compression tests at constant true stress in a temperature range between 1173 and 1323 K in air. The alloys were tested in the cast condition (containing various amounts of the metastable phases Al_5Ti_3 and h-Al_2Ti) and after annealing at 1223 K for 200 h which produced (thermodynamically stable) lamellar γ-TiAl + r-Al_2Ti microstructures. In general, already the as-cast alloys exhibit a reasonable creep resistance at 1173 K. Compared with $Al_{60}Ti_{40}$, both, the as-cast and the annealed $Al_{62}Ti_{38}$ alloy exhibit better creep resistance up to 1323 K which can be rationalized by the reduced lamella spacing. The assessment of creep tests conducted at identical stress levels and varying temperatures yielded apparent activation energies for creep of Q = 430 kJ/mol for the annealed $Al_{60}Ti_{40}$ alloy and of Q = 383 kJ/mol for the annealed $Al_{62}Ti_{38}$ material. The latter coincides well with that of Al diffusion in γ-TiAl, whereas the former can be rationalized by the instability of the microstructure containing metastable phases.

1. Introduction

In previous decades Ti-rich Ti-Al-based intermetallic alloys have been developed successfully as materials for high temperature structure applications because of their low density and high specific strength. Favourable creep properties have been achieved for alloys with lamellar microstructures of γ-TiAl and the Ti-rich α_2-phase [1, 2]. Ti-Al alloy systems with increased aluminium content are expected to result in a significant additional weight reduction and a higher oxidation resistance, due to

the formation of an adherent Al_2O_3 scale [3]. Furthermore, Al-rich Ti-Al alloys offer adequate strength at high temperatures, which would enable them to be used at significantly higher temperatures than Ti-rich γ-Ti-Al-based alloys. During investigations of the phase equilibria in the Al-rich part of the Ti-Al system Palm et al. [4-6] found that lamellar γ-TiAl + r-Al_2Ti microstructures can be generated by means of heat treatment and that the mechanical properties of these alloys could be improved by the formation of lamellar microstructure. Based on these findings an elaborate investigation has been started which aims at the production and detailed characterization of two-phase microstructures of γ-TiAl + r-Al_2Ti and a subsequent evaluation of the resulting mechanical properties.

2. Experimental

Centrifugal casting with Induction Skull Melting technology has shown high potential for manufacturing γ-TiAl components [7]. Hence, test bars of $Al_{60}Ti_{40}$ and $Al_{62}Ti_{38}$ were produced with this technology by ACCESS in Aachen. In general, the alloys showed good melting and casting behaviour. Nevertheless, some pores have been found by non-destructive x-ray inspection in the centre line of the test bars in the as cast condition, probably caused by uncontrolled solidification initiated by a high thermal gradient. The microstructure of the alloys in the as-cast state and after annealing was studied by light-optical, scanning (SEM) and transmission electron microscopy (TEM) and X-ray diffraction (XRD) analyses. Elevated temperature mechanical properties were characterised with compression creep tests on a screw-driven Zwick Z 100 testing machine at temperatures ranging from 1173 to 1323 K in air. The specimens were 5.5 mm high and 3.1 x 3.8 mm² in cross section and were prepared from the cast bars via electro-erosion and subsequent grinding and polishing of the parallel load-bearing surfaces to minimize friction.

3. Results and Discussion

Optical microscopy and XRD analysis of the $Al_{60}Ti_{40}$ and $Al_{62}Ti_{38}$ alloys in the as-cast condition showed a single-phase γ-TiAl microstructure which would contradict the phase diagram [6]. In-depth characterization of the microstructure of the $Al_{60}Ti_{40}$ alloy by TEM revealed a γ-TiAl matrix with domains of the metastable phase Al_5Ti_3 (5-10 nm domain size). The very small size of these Al_5Ti_3 domains results in a pronounced x-ray diffraction peak broadening. Because of the small size it was, thus, impossible to detect these nano-sized second phase particles by XRD analysis. The $Al_{62}Ti_{38}$ alloy showed a more complex microstructure. There are two different orientations of slabs of the metastable h-Al_2Ti phase in the γ-TiAl matrix. The interfaces between both h-Al_2Ti versions are {310} twin surfaces. The investigation revealed also domains of the metastable Al_5Ti_3 phase in addition to the Al_2Ti phase and the γ-TiAl matrix.

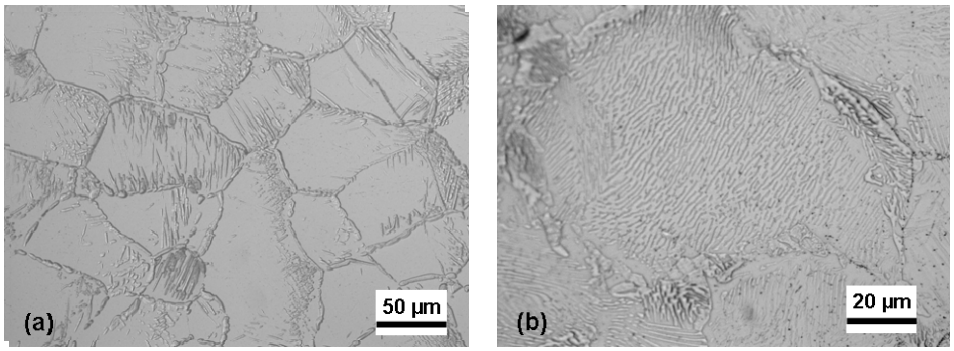

Figure 1. (a) Optical micrograph of the nearly lamellar γ-TiAl + r-Al_2Ti microstructure in $Al_{60}Ti_{40}$ and (b) fully lamellar microstructure of $Al_{62}Ti_{38}$ after annealing

After heat treatment at 1223 K for 200 h and water quenching [4] the microstructure of $Al_{60}Ti_{40}$ was transformed to a relatively coarse, nearly lamellar microstructure of the two phases γ-TiAl and r-Al_2Ti (Figure 1a), which were expected to form in accord with the phase diagram. The $Al_{62}Ti_{38}$ alloy was

annealed at 1223 K for 50 h and water quenched [4]. Here the microstructure changed to a fine lamellar microstructure of the same two phases (Figure 1b).

The minimum creep rate obtained from constant true stress tests and the steady state stress obtained from constant strain rate tests were plotted in a double-logarithmic form in Figure 2 for $Al_{60}Ti_{40}$ [8] and $Al_{62}Ti_{38}$, respectively, in the as cast and the annealed condition at 1273 and 1323 K.

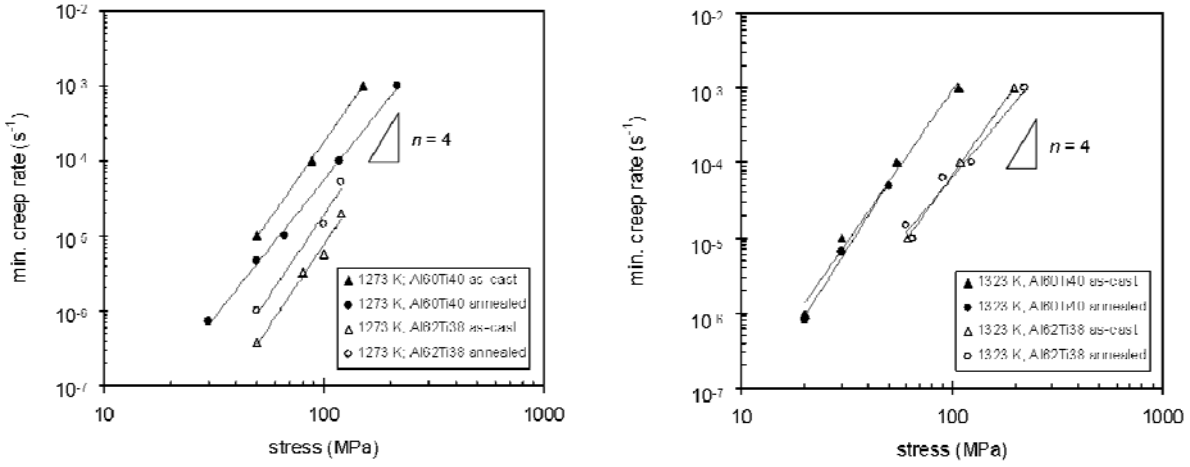

Figure 2. Comparison of secondary creep rates at 1273 K (left) and 1323 K (right) for the $Al_{60}Ti_{40}$ alloy (full symbols) [8] compared with data for the $Al_{62}Ti_{38}$ alloy (open symbols).

Compared with the creep results for the nearly lamellar $Al_{60}Ti_{40}$ alloy [8] it is obvious that both, the as-cast and the annealed $Al_{62}Ti_{38}$ alloy exhibit better creep resistance up to 1323 K. There is no significant difference in the creep behaviour of the as-cast and the annealed condition for both alloys. It should be mentioned that the high Al content of this alloys also provides a very good oxidation resistance which made testing in air possible. Even though the microstructures of all tested conditions are substantially different, the creep strength does not reflect this microstructural variation: with a value of approximately n = 4 the stress exponents were found to be relatively constant in the temperature and stress regime investigated. This value is within the range of n = 3-6 which is predicted by various creep models available in the literature [9-12]. This indicates that dislocation climb may be the rate controlling creep mechanism. In order to determine the activation energy of creep utilizing multiple linear regression, additional compressive creep data were plotted together as the logarithm of the minimum creep rate normalized with temperature vs. the stress normalized with shear modulus according to

$$\dot{\varepsilon} = A(\frac{\sigma}{E})^n \exp(-\frac{Q}{RT}) \quad . \tag{1}$$

The activation energy was varied until an optimal fit (maximum R^2) for the regression was found. The results of these calculations are shown in Table 1. The value for creep of the as-cast $Al_{60}Ti_{40}$ alloy is much higher than the values for interdiffusion of Al or Ti in γ-TiAl found in the literature [12], whereas the value of Q = 383 kJ/mol obtained for the annealed $Al_{62}Ti_{38}$ material coincides well with that of Al diffusion in γ-TiAl [12]. The relatively high observed activation energies may be rationalized by the fact that a metastable two-phase microstructure is present in the $Al_{60}Ti_{40}$ alloy.

Table 1: Activation energy for creep

	$Al_{60}Ti_{40}$ as-cast	$Al_{60}Ti_{40}$ annealed	$Al_{62}Ti_{38}$ as-cast	$Al_{62}Ti_{38}$ annealed
Q_{creep}	550 kJ/mol	430 kJ/mol	385 kJ/mol	383 kJ/mol

A TEM bright-field image of the microstructure creep deformed $Al_{60}Ti_{40}$ as-cast alloy is shown in Figure 3a which prooves the formation of a fine subgrain microstructure. This indicates the dissolution of the metastable Al_5Ti_3 phase during creep deformation and is a possible explanation for the observed high activation energy in the as-cast $Al_{60}Ti_{40}$ alloy. By contrast, the activation energy for creep of the $Al_{62}Ti_{38}$ alloys in both conditions are in the range of the activation energies usually observed for fully lamellar Ti- rich Ti-Al alloys (see for example [13]) where interface related creep phenomena as well as the degradation of the microstructure due to recrystallization and phase transformation determine the creep strength and the activation energy. The $Al_{62}Ti_{38}$ alloy shows the same deformed microstructure for the as-cast and the annealed condition with extended low angle grain boundaries formations and dislocations in globular r-Al_2Ti and γ-TiAl (with precipitates of Al_5Ti_3), shown in Figure 3b. Furthermore the investigation revealed areas of lamellar r-Al_2Ti + γ-TiAl microstructure. Here the dislocations were found only in the γ-TiAl phase, Figure 3c. The results of the TEM investigation may serve as a plausible explanation for the nearly similar creep behaviour for the as-cast and annealed condition of the alloy.

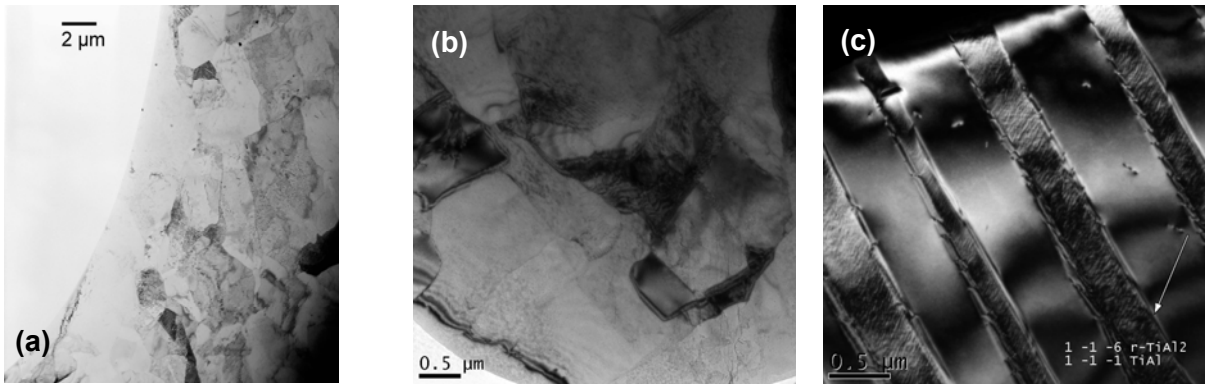

Figure 3. (a) TEM image of the dislocation substructure of $Al_{60}Ti_{40}$, as-cast state, after creep at 1323 K, σ = 60 MPa, ε = 12 % [8]; (b) bright field image of low angle grain boundaries formation of $Al_{62}Ti_{38}$ after creep deformation at 1273 K, σ = 50…100…120 MPa (stress change test), ε = 20 % and (c) dark field image of dislocations in the lamellar γ-TiAl phase in $Al_{62}Ti_{38}$ after creep deformation at 1273 K, σ = 50…100…120 MPa (stress change test), ε = 20 %

Acknowledgements
We gratefully acknowledge financial support from the German Science Foundation (DFG) for funding the group research project Al-rich Ti-Al alloys (PAK 19).

References
[1] Dietrich M 2002 *Titan-Aluminium-Legierungen – eine Werkstoffgruppe mit Zukunft* **1-131**
[2] Clemens H and Kestler H 2000 *Adv. Eng. Mater.* **2** 551-570
[3] Eckert M et al. 1997 *Oxidation of Intermetallics* Wiley-VCH
[4] Zhang L C, Palm M, Stein F and Sauthoff G 2001 *Intermetallics* **9** 229-238
[5] Stein F, Zhang L C, Palm M and Sauthoff G 2001 *Structural Intermetallics* **495-504**
[6] Palm M, Zhang L C, Stein F and Sauthoff G 2002 *Intermetallics* **10** 523-540
[7] Blum M et al. 2002 *Mater. Sci. Eng.* **329-331** 616-620.
[8] Sturm D et al 2009 *Mater. Sci. Eng.* A **510-511** 373-376.
[9] Barrett C R and Nix W D 1965 *Acta Metall.* **13** 1247-1258.
[10] Frost H J and Ashby M F 1982 *The Plasticity and Creep of Metals and Ceramics* (Pergamon Press)
[11] Karthikeyan S, Viswanathan G B and Mills M J 2004 *Acta Mater.* **52** 2577-2589.
[12] Mishin Y and Herzig C 2000 *Acta Mater.* **48** 589-623.
[13] Appel F, Oehring M and Wagner R 2000 *Intermetallics* **8** 1283